NMR and polymorphism of a piperidinone-substituted benzopyran with a fluorinated sidechain

Susan C. Campbell,[a] Robin K. Harris,*,†,[a] Martin J. Hardy,[b] David C. Lee[b] and David J. Busby[b]

[a] *Department of Chemistry, University of Durham, South Road, Durham, UK DH1 3LE*
[b] *SmithKline Beecham Pharmaceuticals, New Frontiers Science Park (North Site), Harlow, Essex, UK CM19 5AW*

Two polymorphs of (3*S*-*trans*)-1-[3,4-dihydro-3-hydroxy-2,2-dimethyl-6-(pentafluoroethyl)-2*H*-1-benzopyran-4-yl]piperidin-2-one (A)‡ have been characterised by solid-state ^{13}C and ^{19}F cross-polarisation magic-angle spinning NMR, aided by IR spectroscopy, differential scanning calorimetry and X-ray powder diffraction methods. The two polymorphs show markedly different NMR spectral phenomena, including variations in residual dipolar coupling characteristics and crystallographic splitting of resonances, indicating that more than one molecule exists in the asymmetric unit of polymorphic form II. The ^{13}C NMR studies involved triple-channel operation, with simultaneous decoupling of ^{1}H and ^{19}F, including cross polarisation from ^{19}F as well as from ^{1}H. Dual-channel ^{19}F measurements have been carried out using ^{1}H decoupling, with cross polarisation from ^{1}H.

Introduction

The aim of this paper is to present recent results obtained by applying novel ^{19}F{^{1}H} and triple-channel ^{13}C{^{1}H,^{19}F} CP MAS NMR techniques to two polymorphs of compound **A**, the molecular structure and atomic numbering scheme of which are shown below.

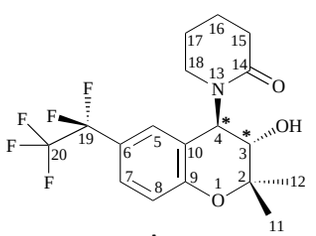

A

* = Chiral centres

Atomic structure and numbering of A

In recent years, increasing recognition of the gravity of polymorphism issues[1–4] in the pharmaceutical industry has led to the identification of techniques[5] which provide accurate methods for characterisation of individual forms. This has implications for acceptable sample purity, since differences in the bioavailability of different polymorphic forms may have major consequences, and also increasingly for patent law, since the identification of individual polymorphs may assist with prolonging intellectual property rights and patents on particular products. Solid-state NMR is increasingly becoming recognised as the technique of choice for identifying and characterising polymorphs and their mixtures.[6] Following initial indications of polymorphism in **A** provided by infrared microspectrometry and differential scanning calorimetry, a solid-state NMR study has been implemented to identify the polymorphs of **A** and to probe the differences in the structure between the forms.

Magic-angle spinning (MAS) ^{19}F NMR spectra of partially fluorinated solid organic compounds are difficult to obtain with high resolution for two main reasons. Firstly, strong dipolar (H,F) interactions are likely to exist, which cannot be simply overcome by MAS because of complications resulting from strong homogeneous (H,H) dipolar coupling. High-power proton decoupling is therefore necessary, but work in this area has been inhibited by the fact that ^{1}H and ^{19}F resonance frequencies differ by only *ca*. 6%, so that highly-efficient frequency isolation is required. However, ^{19}F{^{1}H} spectra for organic solids with isolated fluorine nuclei have recently been obtained successfully.[7,8] The second problem arises when the solid system contains fluorine atoms in close spatial proximity, thus giving rise to strong (F,F) dipolar interactions. Since these are homogeneous in nature, MAS is not as efficient an averaging technique as it is for heteronuclear dipolar interactions and for shielding anisotropy. Either very fast MAS or combined rotation and multiple pulse spectroscopy (CRAMPS) is required.[9–11] One aim of the work reported here was to see to what extent a combination of modest MAS rates (*ca*. 10 kHz) combined with high-power proton decoupling would suffice to give ^{19}F spectra capable of distinguishing between polymorphs containing perfluoroethyl groups. Obviously, ^{19}F spectra can be obtained much more rapidly than natural-abundance ^{13}C spectra and so in principle may be preferred for polymorph identification and quantitative analysis.

However, in most polymorphic systems of pharmaceutical interest, the number of fluorine atoms in the molecule is likely to be relatively small, so that more detailed information should be available from ^{13}C cross-polarisation (CP) MAS spectroscopy. Here, too, the existence of fluorines constitutes a drawback to obtaining high-resolution spectra with conventional techniques, *i.e.* with two-channel spectrometers using proton decoupling. In the first place ^{19}F, ^{13}C isotropic indirect coupling can complicate spectra. Secondly, the effects of homogeneous ^{19}F, ^{19}F dipolar interactions result in broadened ^{13}C lines at modest MAS rates. Of course, high-power continuous-wave or multiple-pulse ^{19}F decoupling can overcome both problems, but clearly when protons are also present in the molecule this requires triple-channel ^{13}C{^{1}H,^{19}F} operation. Suitable spectrometers and probes have only recently become available, but few applications to systems of pharmaceutical interest have yet been reported.

† E-Mail: r.k.harris@durham.ac.uk
‡ *trans* Refers to the relative orientation of the 3- and 4-substituents.

Thus, as in the case of solid **A**, assignment of $^{13}C\{^{1}H\}$ spectra may prove to be problematic, and although spectral editing techniques such as dipolar dephasing[12–14] (non-quaternary suppression) may be used, it is obviously desirable to apply double-decoupling techniques[15–17] in order to remove splittings due to (^{19}F,^{13}C) indirect coupling and to reduce the linewidths of the resonances in the spectra which, due to their broadness, will otherwise severely overlap. A triple-channel $^{1}H/^{19}F/^{13}C$ (HFX) probe is of considerable use when observing such highly fluorinated and protonated molecules. Furthermore, it allows cross polarisation from ^{19}F to ^{13}C (as well as the more usual ^{1}H to ^{13}C CP), which can be of value in establishing the proximity of such nuclei. This is particularly useful for **A**, where the proton cross-polarisation efficiencies to the fluorinated carbon atoms remote from proton nuclei are very low. Thus the HFX probe may be used to acquire spectra which are markedly different to those acquired on a dual-channel, proton/carbon probe.

Experimental

Preparation

During the synthetic route development to **A**, two different methods were used for the final purification and isolation procedures. These resulted in the preparation and identification of two distinct crystalline forms of **A**, which have been designated as forms I and II. Form I is obtained by recrystallisation of **A** from diisopropyl ether followed by drying under a vacuum. Form II is prepared by dissolution in ethyl acetate, followed by evaporation to dryness in a vacuum. The resulting solid is triturated with hexane, filtered off, washed again with hexane and dried under a vacuum. Attempts to form single crystals were made, but without success due to the microcrystalline nature of the sample.

Table 1 ^{1}H Solution-state NMR assignments[a]

δ_H	Assignment[b]	J/Hz
7.38	7	$^{4}J_{5,7} = 2.3$
7.16	5	
6.91	8	$^{3}J_{7,8} = 8.6$
5.96	4	$^{3}J_{3,4} = 10.2$
4.16	OH	
3.78	3	
3.14	18	
2.86	18′	
2.58	15, 15′	
1.88	16, 16′	
1.84	17	
1.67	17′	
1.53	CH_3(eq)	
1.27	CH_3(ax)	

[a] In $CDCl_3$. [b] See structure of **A**.

NMR

The materials were characterised by solution-state ^{1}H and ^{13}C NMR (Tables 1 and 2) and found to be pure chemically. A Varian VXR400 spectrometer operating at 9.4 T was used (^{13}C at 100.58, and ^{1}H at 399.96 MHz). CP MAS NMR spectra[18] were obtained using a Chemagnetics CMX200 spectrometer operating at 4.7 T (^{13}C at 50.33, ^{1}H at 200.13 and ^{19}F at 188.29 MHz). Samples used for ^{13}C spectra were housed in 7 mm zirconia pencil rotors and spun at *ca*. 6 kHz with a specially-designed HFX triple-channel probe. A 20 kHz spectral width and 3 s recycle delay were used for $^{13}C\{^{1}H\}$ proton-to-carbon cross polarisation. A 3 s recycle delay was also required for ^{19}F to ^{13}C CP since the ^{19}F spin-lattice relaxation times were measured as 0.62 s (form I) and 0.47 s (form II). Fluorine-19 MAS NMR was carried out using a $^{1}H/^{19}F$ CP contact time of 10.0 ms, with a sample spinning speed of 10 kHz and 4 mm zirconia rotors; a recycle delay of 3 s was used for both CP and single pulse experiments. The experiments were carried out using a Chemagnetics HF probe[19] with a ^{19}F RF trap to prevent breakthrough of the proton decoupling frequency into the fluorine channel.

Solution-state ^{1}H and ^{13}C chemical shifts are given with respect to the relevant signal for internal tetramethylsilane directly, while solution-state ^{19}F shifts are referenced to the fluorine resonance of $CFCl_3$.

Solid-state carbon-13 chemical shifts were referenced to the high-frequency adamantane resonance at 38.4 ppm, by replacement, and ^{19}F shifts are quoted with respect to the signal for liquid $CFCl_3$. With a proton decoupling power of 100 kHz the Bloch–Siegert shift[10] for $^{19}F\{^{1}H\}$ experiments can be calculated to be approximately −2 ppm.

Table 2 Comparison of ^{13}C solution-state NMR assignments with CP MAS and NQS experiments of both polymorphs of **A**

Assignment[a]	Solution[b]		Solid state	
	δ_C	J[c]/Hz	Form I δ_C	Form II[d] δ_C
14	173.7		172.9	178.0, 173.4, 171.2 RDC[e]
9	157.3		157.8	158.4, 156.9 (155.0)[f]
7	127.3	$^{3}J_{CF} = 6.0$	126.7	127.7
8	118.1		124.0	126.3
5	125.8	$^{3}J_{CF} = 6.3$	121.3	123.6
6	120.9	$^{2}J_{CF} = 24.8$	121.0	121.0
10	120.3		119.3	120.1
20	119.2	$^{1}J_{CF} = 285.9$ $^{2}J_{CF} = 40.3$	118.7	119.3
19	113.5	$^{1}J_{CF} = 253.6$ $^{2}J_{CF} = 38.1$	114.3	113.6
2	80.2		81.1	80.8, 79.0 (1:2)
3	70.8		67.7	70.6, 68.0, 67.2
4	53.8		52.7	55.4–51.8 RDC[e]
18	42.7		42.3	43.5–39.3 RDC[e]
15	32.4		34.1	33.5, 31.9 (2:1)
CH_3 (eq)	26.7		26.7	27.7, 26.6 (1:2)
17	23.1		24.0	24.5, 23.1 (2:1)
16	21.0		20.5	21.7
CH_3 (ax)	18.2		18.6	20.0, 19.0 (2:1)

[a] See structure of **A**. [b] In $CDCl_3$. [c] J = Scalar couplings. [d] Relative intensities given in parentheses. [e] RDC = Residual Dipolar Coupling. [f] Possibly from an impurity.

The magic angle was set by optimising the signal for KBr to obtain the greatest number of rotational echoes in the free induction decay.[20]

Differential scanning calorimetry, infrared spectroscopy and powder X-ray diffraction

DSC and IR measurements were obtained at SmithKline Beecham Pharmaceuticals, Harlow. These were used for identification purposes. The conversion of form I into form II can be induced thermally (the reverse transformation has not been observed). FTIR spectra were obtained from Nujol mulls using a Perkin-Elmer 1750 FTIR spectrometer (2 scans, interleaved mode, 4 cm^{-1} resolution). The spectrometer was purged with dry air. DSC data were collected on a Perkin-Elmer DSC-2C instrument using heating rates of 10 °C min^{-1} over a temperature range from 30 °C upwards. An atmosphere of nitrogen at a flow rate of 5 ml min^{-1} was used.

Powder X-ray diffraction was carried out using a software-controlled Philips PW1050 powder diffractometer. The software was called 'Traces', and was designed by Diffraction Technology, 38 Essington St., (PO Box 444), Mitchell, ACT, 2911, Australia.

Results and discussion

The results of DSC and IR measurements will be presented first, as they provided the initial demonstration of the existence of the two polymorphic forms of compound **A**.

DSC traces of forms I and II are shown in Fig. 1. Both show relatively sharp melting endotherms with onsets of 150 and 147 °C respectively. These onset temperatures are fairly typical of the two forms, although for some batches of form I the onset of melting has been observed around 151 °C. No thermal events are observed on cooling the melt, which solidifies to form a glass. Fig. 1 also shows the DSC trace of the glass obtained from the melt of form I [as expected, the glass derived from form II gives essentially the same trace (data not shown)]. The small endothermic drift around 50 °C is believed to be a glass transition. The broad exotherm over the range 90–120 °C corresponds to crystallisation, which is followed by melting (onset 147 °C). This is consistent with the formation and melting of form II (this was subsequently confirmed by variable temperature IR studies). To summarise, melting, cooling and reheating either form produces form II.

The IR spectra of the two forms show extensive differences (Fig. 2). Form I has a single O–H stretching band at 3436 cm^{-1}, whereas form II shows a complex envelope between 3600 and 3100 cm^{-1} (principal bands at 3428 and 3209 cm^{-1}). The carbonyl stretching region reflects the hydroxy stretching region to some extent, with form I displaying a single band at 1619 cm^{-1} and form II displaying principally two bands at 1643 and 1607 cm^{-1}. Clearly the hydrogen-bonding is significantly different in the two forms, with greater complexity in form II. Significant differences also occur around 1200 cm^{-1} (asymmetric C–O–C stretching in the chroman ring); form I displays a single intense band at 1206 cm^{-1} and form II shows two intense bands at 1214 and 1201 cm^{-1}. C–F stretching is expected to give rise to several strong bands between 1400 and 1100 cm^{-1}, but vibrational coupling with the aromatic ring makes unambiguous assignment difficult. The coupled out-of-plane deformation of the two adjacent aromatic hydrogens gives absorption near 830 cm^{-1}, which is again split into two components in the case of form II. Below 800 cm^{-1} the spectra of both forms are relatively similar.

Powder X-ray diffractograms confirmed that the two polymorphs are, indeed, crystallographically very different (Fig. 3).

The room-temperature ^{1}H–^{13}C CP MAS spectra for polymorphic forms I and II are shown in Fig. 4. These spectra show marked differences. That of form II contains extensive crystallographic splitting of many signals, indicating the existence of more than one molecule in the asymmetric unit. Splittings into two peaks are particularly clear for the resonances of C(2) at ~80 ppm, C(15) at ~33 ppm and CH_3 (eq) at ~27 ppm with approximately 1:2 or 2:1 relative intensities, though the band assigned to C(3) is split into three distinct peaks (70.6, 68.0, 67.2 ppm) which may indicate, along with the complex shape of the resonances for C(14) (see below), the presence of three chemically distinct molecules in the asymmetric unit.

(^{13}C, ^{14}N) dipolar coupling interactions,[21,22] which are not averaged out by the rapid MAS, manifest themselves in the

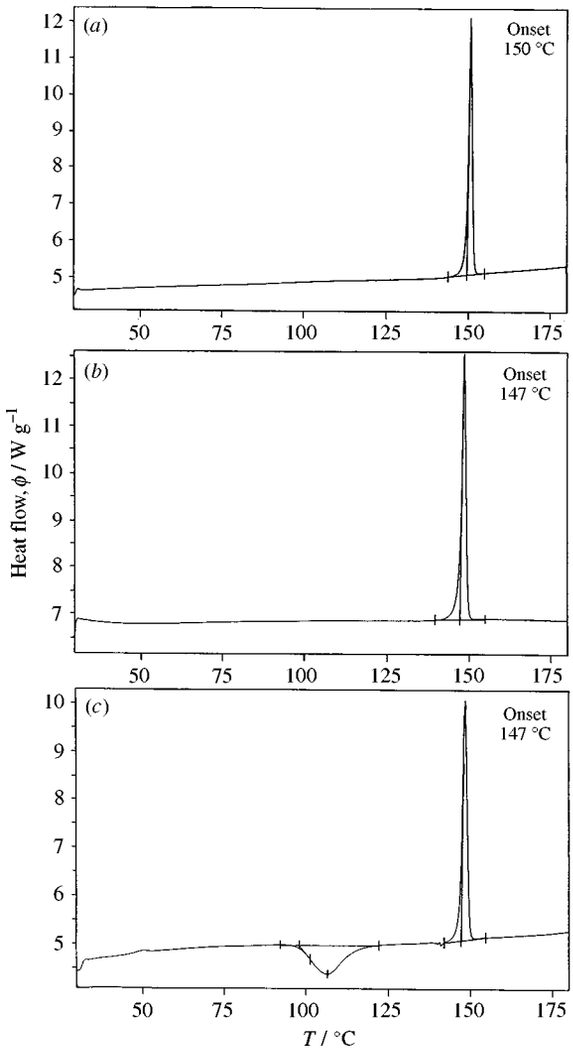

Fig. 1 DSC traces of (*a*) form I and (*b*) form II and (*c*) the glass obtained from cooling the melt of form I

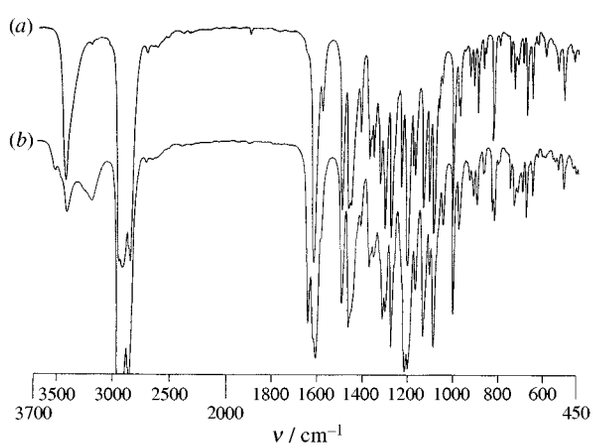

Fig. 2 Infrared spectra of Nujol mulls of (*a*) form I and (*b*) form II

Table 3 Comparison of ^{13}C, ^{14}N residual dipolar splittings (*s*) at 50 MHz for selected ribonucleosides and form II of compound **A**

Reference molecule	^{13}C–^{14}N	^{13}C [a]	r_{C-N}/Å	β^D	s/Hz [d]	
					Literature	Experimental [e]
Cytidine [b]	C(2)–N(1)	14	1.379	90	78	83
	C(6)–N(1)	18	1.368	90	79.5	95
	C(1)–N(1)	4	1.497	90	60.5	65
Uridine [c]	C(2)–N(1)	14	1.371	90	86	83
	C(6)–N(1)	18	1.369	90	86.5	95
	C(1)–N(1)	4	1.490	90	67	65

[a] Identifies the ^{13}C–N bond in compound **A** most similar to the given C–N bond in the reference molecule. [b] Cytidine N(1): $\chi = -3$ MHz, $\eta = 0$. [c] Uridine N(1): $\chi = -3.28$ MHz, $\eta = 0.02$. [d] In all cases quoted, *s* is positive (*i.e.* a 1:2 doublet is seen). [e] This work.

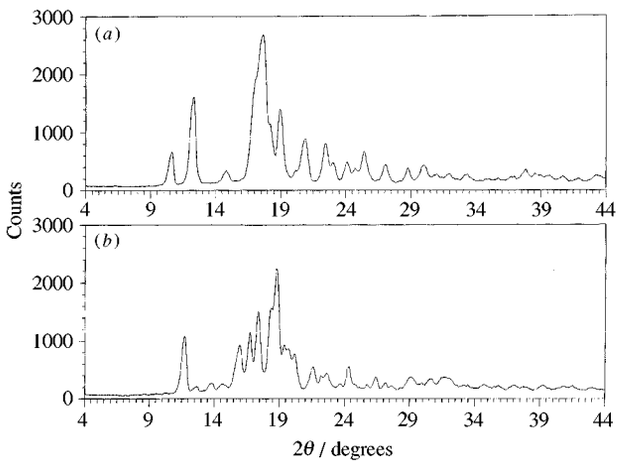

Fig. 3 Powder X-ray diffraction traces of (*a*) form I and (*b*) form II

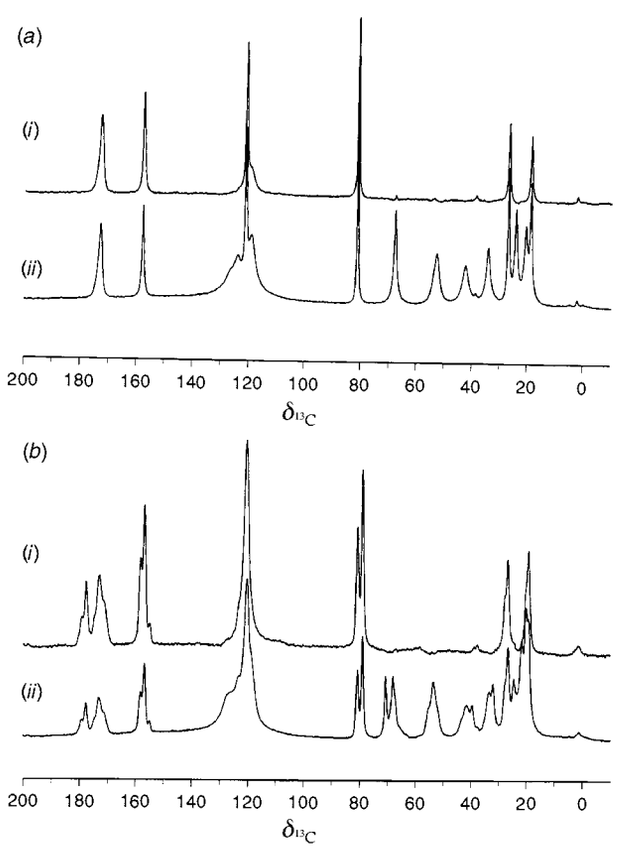

Fig. 4 Solid state ^{13}C CP MAS NMR spectra of (*a*) form I and (*b*) form II comparison of (*i*) CP with flip-back and (*ii*) non-quaternary suppression experiment (10016 transients, 2.0 ms contact time, 3.0 s recycle delay, 50 μs dephasing time, 6 kHz sample spinning speed)

form of asymmetric doublets of intensity ratio 1:2 or 2:1. This residual dipolar splitting exists for resonances assigned to carbons (14), (18) and (4), which are directly bound to the nitrogen atom. In the spectra of form II, the splitting is very pronounced, and is especially evident in the case of C(14), which shows asymmetric bands at 178 and 173 ppm. In the spectra of form I, however, this effect only contributes to the broadening of this particular resonance.

The splittings and/or broadenings for resonances of C–N carbons were confirmed as arising from residual dipolar interactions by observation of spectra obtained at higher magnetic field (Varian Unity Plus 300 spectrometer), which show reduced splittings and/or narrower peaks.

The signal at *ca*. 178 ppm for C(14) in form II is a clear 1:2 doublet. However, the band at *ca*. 173 ppm is more complex in shape, and we believe it to consist of two overlapping 1:2 doublets. This is reflected in the data given in Tables 2 and 3. The chemical shifts given for C(14) of form II in Table 2 are the true values based on the weighted averages of the 1:2 doublets, whereas only ranges of absorption are listed for C(4) and C(18). Calculation of the residual dipolar coupling can be carried out using the first-order perturbation eqn. (1), where *s* is the

$$s = \left(\frac{9}{20}\right)\left(D\,\frac{\chi}{Z_N}\right)(3\cos^2\beta^D - 1 + \eta\sin^2\beta^D\cos 2\alpha^D) \quad (1)$$

doublet splitting, *D* is the dipolar (^{13}C, ^{14}N) coupling constant, χ is the ^{14}N quadrupole coupling constant, Z_N is the ^{14}N resonance frequency at the applied magnetic field, and η is the asymmetry parameter of the ^{14}N electric field gradient (EFG). α^D and β^D are the polar angles defining the orientation of the internuclear vector ***r*** in the EFG.

A comparison of the observed splittings (*s*) for form II was made with those quoted in the literature [23,24] for the ribonucleoside molecules cytidine and uridine. The 'N(1)' atoms in those compounds show a similar chemical configuration to the N(13) present in compound **A**. It is assumed that the *z* axis of the quadrupole tensor points along the lone pair orbital which is taken to be perpendicular to the NR_3 group (assumed to be essentially planar), therefore causing the angle β^D to be 90°. The asymmetry parameter η is assumed to be zero, implicitly causing the angle α^D to be irrelevant. The individual r_{N-C} values were taken from the appropriate N–C distances in the ribonucleosides and χ is taken to be approximately −3 MHz.

Our splitting magnitudes for form II seemed to be of similar order to those given in the literature (see Table 3), although the larger values observed in our experiments seem to suggest that our χ values may be slightly greater, or to imply that C–N bond lengths in compound **A** may be shorter than those extracted from the literature. The most extreme difference is for the C(18)–N bond which therefore is probably significantly shorter than the N(1)–C(6) bond in the two ribonucleosides. Of course, the relevant ^{13}C signals are powder patterns, so that values of *s* are subject to significant errors (*ca*. 8 Hz).

The observation of three asymmetric doublets of 1:2 inten-

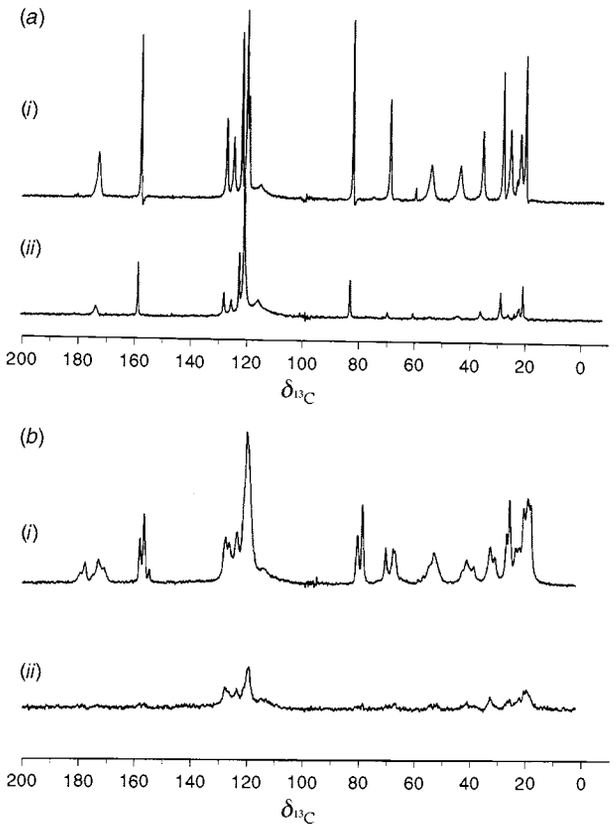

Fig. 5 ^{13}C CP MAS NMR spectra of (*a*) form I and (*b*) form II of (**A**) using simultaneous ^{1}H and ^{19}F broadband decoupling during acquisition and (*i*) proton-to-carbon, (*ii*) fluorine-to-carbon cross polarisation (2884 transients, 10.0 ms contact time, 3.0 s recycle delay, 5 kHz sample spinning speed)

sity for the C(14) resonance for form II may be explained by the existence of three molecules in the crystallographic asymmetric unit (as mentioned above). Surprisingly, no residual dipolar splitting is visible for the C(14) signal of form I, possibly because of unfavourable angles a^D and β^D.

A broad area of indistinguishable peaks which is very difficult to resolve can be observed around 120 ppm. On the basis of solution-state spectral assignments this may be attributed to the fact that there are possibly seven individual resonances occurring for form I in this region. These include the signals for quaternary carbons (6) and (10); fluorinated carbons (19) and (20); plus the protonated aromatic carbon resonances (5), (7) and (8).

Dipolar dephasing experiments (Fig. 4) were carried out in order to identify the quaternary and methyl carbon atoms.

Triple-channel HFX experiments were carried out with high-power continuous-wave proton and fluorine decoupling. This increased the resolution of the 120 ppm region although seven peaks were still not discernible for form I (Fig. 5). Fluorine-to-proton cross polarisation was then implemented, with interesting results (Fig. 5). Both forms I and II now displayed broad peaks at approximately 114 ppm, which may be attributed to the CF_2 group, C(19), and which were not evident in previous proton-to-carbon CP spectra. A background spectrum of an empty rotor was run and subtracted from the spectra in order to verify that this peak was not arising from fluorinated components in the rotor or the probe. Greater resolution than for ^{1}H–^{13}C CP was also achieved, most noticeably for form II, where five more peaks may now easily be recognised in the 120 ppm region. Variable contact time CP MAS experiments were used to elucidate the signals for protonated carbons (5), (7) and (8), whose lower T_{CH} values cause these resonances to occur after a shorter cross polarisation time within the poorly resolved region around 120 ppm.

Table 4 Comparison of ^{19}F chemical shifts of the two polymorphs

	δ_F [a]	
Assignment	Form I	Form II
CF_3	−87.0	−88.2
CF_2	−117.8	−112.6
	−119.1 [b]	−117.0
		−120.3

[a] Uncorrected for the Bloch–Siegert shift which is expected to be *ca.* −2 ppm. [b] Shoulder (see Fig. 6).

The final assignments of the ^{13}C CP MAS spectra, which were made using the combination of non-quaternary suppression, variable contact time, and triple-channel experiments, are displayed in Table 2.

The largest variations in the chemical shifts of individual ^{13}C nuclei seem to occur for atoms which may be involved in either inter- or intra-molecular hydrogen bonding. This includes carbon atoms (14) and (3). Both signals show large inter-form variations as well as large individual deviations from the isotropic, solution-state values. The results appear to suggest strong intramolecular hydrogen-bonding, or a different conformation about the C(14)–N bond, for one of the independent molecules of form II only, giving a high frequency shift of *ca.* 5 ppm.

Low-temperature work on both polymorphs shows no significant changes in the solid-state NMR spectra between 198 and 143 K. This indicates that there is no extra information to be gained by working at low temperature for either form.

Fluorine-19 NMR has also been applied to this system, and the AB coupling evident in solution-state NMR of this compound is replicated by the broadness of the signal for C(19) for the solid (Fig. 5). Differences between the spectra of the two polymorphs occur both for the CF_2 resonances (for which form II shows three maxima) and for the CF_3 resonances (Table 4). Although these differences are not great, they are definitive, and they allow distinctions to be made between the samples in much shorter times than is the case for ^{13}C NMR. It is evident that improvements in resolution are necessary if ^{19}F NMR is to become fully useful for **A**, *e.g.* to examine polymorph mixtures. However, high-power proton decoupling has clearly been successful, and the resulting linewidths for the CF_3 signals are commensurate with those we have obtained[7] for systems with well-separated fluorine atoms. Linewidths typically observed for the proton-decoupled CF_3 resonances are *ca.* 420 and 580 Hz for forms I and II respectively.

Fluorine-19 T_1 inversion–recovery experiments with proton decoupling have been carried out by observation of the CF_3 peak giving values of 0.62 (form I) and 0.47 s (form II). Variable spin-lock experiments have also been applied to this system, resulting in the observation of $T_1\rho$ values of 85–105 ms for the fluorine resonances of form I and 170–185 ms for the fluorine resonances of form II. These results are of the orders of magnitudes expected and are valuable in establishing the optimum conditions for proton-to-fluorine-19 cross polarisation experiments.

Proton T_1 values were measured using a cross polarisation version of the Freeman–Hill experiment and found to be 1.24 s (±0.2 s) for both form I and form II.

Conclusions

Initial indications of the existence of polymorphism of **A** have been confirmed by solid-state NMR techniques. By the application of double decoupling to this system, increased resolution of the previously confusing ^{13}C spectrum has been achieved, and this has led to a detailed assignment. The spectra of the two forms are substantially different, partly because form II has

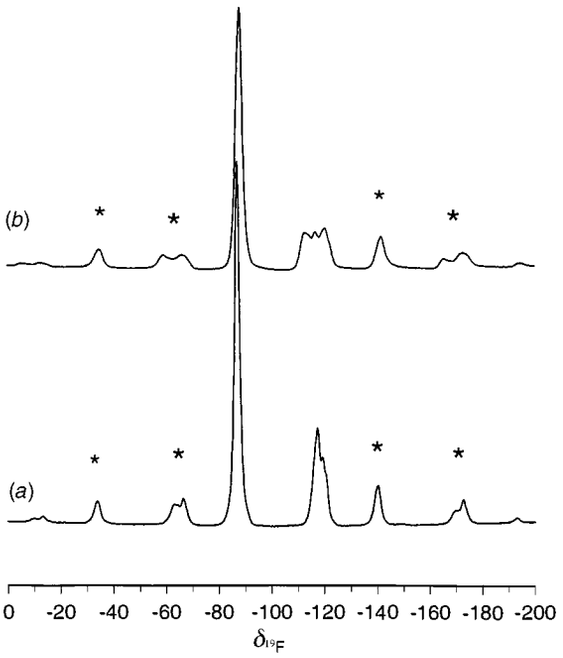

Fig. 6 ^{19}F solid-state CP MAS NMR spectra of (*a*) form I and (*b*) form II of (**A**) using CP with flip back (128 transients, 10.0 ms contact time, 3.0 s recycle delay, 10 kHz sample spinning speed); asterisks indicate spinning sidebands

more than one molecule in the asymmetric unit. However, fluorine-19 spectra, with proton decoupling, have proved to be of only limited use for **A**. DSC and IR studies have also provided evidence of the irreversible conversion of form I to form II on heating.

Acknowledgements

This research was carried out with a spectrometer system purchased using EPSRC research grants GR/H96096 and GR/J97557. One of us (S. C. C.) thanks the EPSRC and SmithKline Beecham Pharmaceuticals for a studentship under the CASE scheme. Our thanks also go to C. W. Lehman at the University of Durham for the XRD experiments.

References

1 S. Byrn, R. Pfeiffer, M. Ganey, C. Hoiberg and G. Poochikan, *Pharm. Res*., 1993, **12**, 7.
2 S. Byrn, R. Pfeiffer, G. Stephenson, D. W. Grant and W. B. Gleason, *Pharm. Res*., 1994, **6**, 1148.
3 J. A. Davies, S. G. Dutremez and A. A. Pinkerton, *Magn. Reson. Chem*., 1993, **31**, 435.
4 D. Casarini, R. K. Harris and A. M. Kenwright, *Magn. Reson. Chem*., 1993, **31**, 540.
5 T. L. Threlfall, *Analyst*, 1995, **120**, 1440.
6 R. K. Harris, 'Polymorphism and related phenomena', in *Encyclopedia of NMR*, ed. D. M. Grant and R. K. Harris, Wiley, Chichester, New York, 1995, vol. 6, pp. 3734–3740.
7 S. A. Carss, PhD Thesis, Durham University, 1995.
8 J. M. Miller, *Prog. Nucl. Magn. Reson. Spectrosc.*, 1996, **28**, 255.
9 R. K. Harris and P. Jackson, *Chem. Rev*., 1991, **91**, 1427.
10 S. A. Vierkotter, *J. Magn. Reson., Ser. A*, 1996, **118**, 84.
11 B. C. Gerstein, 'CRAMPS', in *Encyclopedia of NMR*, ed. D. M. Grant and R. K. Harris, Wiley, Chichester, New York, 1995, vol. 3, pp. 1501–1509.
12 K. W. Zilm, 'Spectral Editing Techniques', in *Encyclopedia of NMR*, ed. D. M. Grant and R. K. Harris, Wiley, Chichester, New York, 1995, vol. 7, pp. 4498–4504.
13 X. Wu and K. W. Zilm, *J. Magn. Reson. A*, 1993, **102**, 205.
14 R. G. Griffin, G. Bodenhausen, R. A. Haberkorn, T. H. Huang, M. Munowitz, R. Osredkar, D. J. Ruben, R. E. Stark and H. van Willigen, *Phil. Trans. R. Soc. Lond. A*, 1981, **299**, 547.
15 J. Schaefer, R. A. McKay and E. O. Stejskal, *J. Magn. Reson.*, 1979, **34**, 443.
16 E. Hagaman, *J. Magn. Reson. A*, 1993, **104**, 125.
17 J. Schaefer, E. O. Stejskal, J. R. Garbow and R. A. McKay, *J. Magn. Reson*., 1984, **59**, 150.
18 R. K. Harris, '*Nuclear Magnetic Resonance – A Physicochemical View*', Longman Scientific and Technical, 1986, ch. 6.
19 U. Scheler, P. Holstein, S. A. Carss and R. K. Harris, *Chemagnetics Applications Lett*., 1995.
20 J. S. Frey and G. E. Maciel, *J. Magn. Reson*., 1982, **48**, 125.
21 S. H. Alarcon, A. C. Olivieri, S. A. Carss, R. K. Harris, M. J. Zuriaga and G. A. Monti, *J. Magn. Reson. A*, 1995, **116**, 244.
22 A. Naito, S. Ganapathy and C. A. McDowell, *J. Magn. Reson.*, 1982, **48**, 367.
23 A. C. Olivieri, L. Frydman, M. Grasselli and L. E. Diaz, *Magn. Reson. Chem*., 1985, **26**, 281.
24 A. C. Olivieri, L. Frydman and L. E. Diaz, *J. Magn. Reson*., 1987, **75**, 50.

Paper 7/03187D
Received 8*th May* 1997
Accepted 19*th June* 1997